Modeling Microwave Chiral Material Based on Cranks Resonator Array Using Comsol Multiphysics

J. Muñoz*[1], G.J. Molina[1], and M. Rojo[1]
[1]University of Murcia
*Corresponding author: Dpto. Electromagnetismo y Electrónica, Universidad de Murcia, Campus de Espinardo, Murcia E-30100, Spain, juanmu@um.es

Abstract: Electromagnetic metamaterials present exotic and unusual properties hardly to be found in nature with many potential applications. They are usually built by distributing small resonant structures in periodical lattices. If the structure has chiral symmetry, the medium is called chiral metamaterial. Here the electrodynamics behaviour of a chiral structure with a huge electromagnetic activity at microwave frequencies is modeled by making use of COMSOL Multiphysics RF module and successfully compared to the experiment. Linearly and circularly polarized modes at normal incidence have been simulated and different experimental conditions have been modeled to extract reflection and transmission coefficients for the electromagnetic characterization of the sample.

Keywords: Chiral metamaterials, microwave measurements, polarization, field computation.

1. Introduction

In the last decade, chiral materials have attracted much attention since it was theoretically predicted that negative refractive index can be achieved for large chiral activity, and, unlike conventional negative index structure designs, the chiral negative index structure does not require simultaneously negative permittivity and permeability.

Chiral media produce two effects on the propagation of a linearly polarized wave: a rotation of the polarization angle, known as electromagnetic rotatory dispersion, and the polarization changes to elliptical, known as circular dichroism.

Moreover, unlike conventional negative index structures designs, for chiral materials only one resonant structure with high electromagnetic activity is necessary to achieve negative refraction index. Thus, several chiral structures have been proposed to obtain large optical activity, circular dichroism and negative refraction with many potential applications, both at microwave and optical frequencies. Further information on this subject is addressed in [1] and [2], and references therein.

In this paper we make use of three dimensional cranks as the basic chiral structure in order to obtain negative refractive index materials. A chiral medium constituted by a periodical lattice of a two-dimensional array of four same handedness three-dimensional metallic cranks patterned on a double side FR-4 dielectric board (Fig. 1) has been reported by the authors [1] to present large electromagnetic activity, circular dichroism, and negative refractive index in the X-band frequency range. The structure clearly lacks of mirror symmetry, possesses C4 symmetry on the perpendicular axis, and presents uniaxial chirality for normal incident TEM wave. Therefore, the electromagnetic activity is not sensitive to the direction of a linearly polarized wave for normal incidence.

Powerful commercial software packages, such as COMSOL Multiphysics finite-element based software, allow to explore the physical behaviour of structures on a computer in order to optimize the design, before to build the real prototype in workshop or laboratory. Thus, cost and effort can be reduced significantly. Here, we have used the RF module of COMSOL 4.2a version to model the electromagnetic behaviour of our structure and to study how it is related with its design. In this process, the simulations have illuminated aspects of the phenomenon that cannot be seen in the laboratory.

2. Basic equations

The macroscopic behaviour of isotropic chiral media can be characterized by the constitutive relations:

$$\vec{D} = \varepsilon_0 \varepsilon_r \vec{E} - j\sqrt{\varepsilon_0 \mu_0}\,\kappa \vec{H}$$
$$\vec{B} = \mu_0 \mu_r \vec{H} + j\sqrt{\varepsilon_0 \mu_0}\,\kappa \vec{E}, \qquad (1)$$

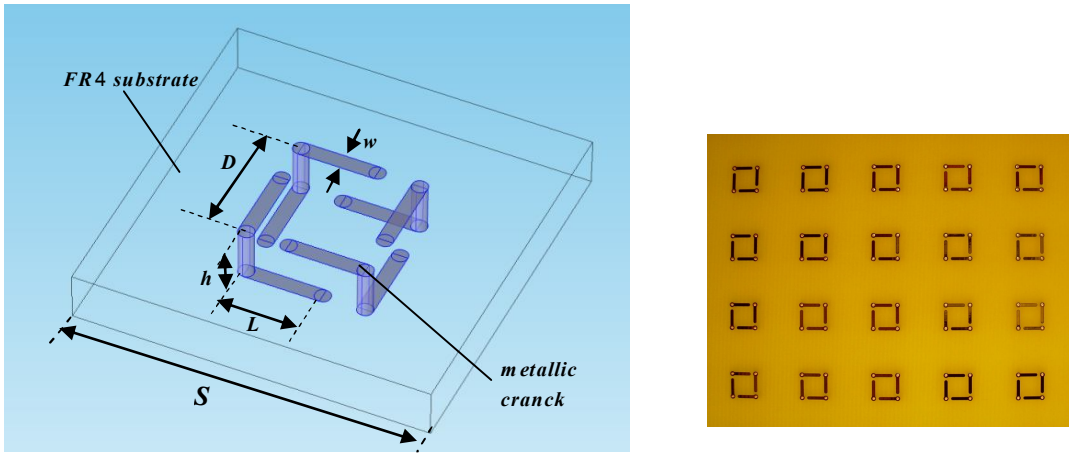

Figure 1. (Left) The four cranks resonator and (Right) a picture of the experimental sample. The geometric parameters are given by S=13.5 mm, D=4.5 mm, L=2.9 mm, h=2.4 mm, and w=0.6 mm. The three dimensional structure is patterned by connecting metallic (copper) segments, 30 μm thick, in both sides of FR-4 dielectric substrate board through via holes.

where ε and μ are the effective electric permittivity and magnetic permeability, respectively, and the chirality parameter, κ, describes the strength of the electric-magnetic cross coupling. Chirality affects the refractive index of the two circularly polarized modes into which the linear incident wave can be split. Each mode spreads through the medium as if it were isotropic, with refractive indices:

$$n_R = n + \kappa, \quad n_L = n - \kappa, \tag{2}$$

where n_R and n_L represent the refractive indices for the right-handed circularly polarized (RCP) and the left-handed circularly polarized (LCP) waves, respectively, and $n = \sqrt{\varepsilon\mu}$ is the conventional defined refractive index. Thus, $|\kappa|$ should be large enough to overcome the magnitude of n to achieve negative n_R or n_L. In our case, the material exhibits a high electromagnetic activity and a relatively low refractive index [1]; the joined effect of both factors results into negative values of the refractive index for the RCP wave in a narrow bandwidth.

The transmission coefficients for the LCP, T_L, and RCP, T_R, modes may be calculated from the transmission coefficients for both components of the electric field, parallel (T_{CO}) and perpendicular (T_{CR}) to the polarization direction of the incident field:

$$\begin{aligned} T_R &= T_{CO} + jT_{CR}, \\ T_L &= T_{CO} - jT_{CR}. \end{aligned} \tag{3}$$

The rotation of the polarization angle, θ, defined as the difference between the polarization direction of the incident wave and the direction of the major axis of the transmitted elliptically polarized wave; the ellipticity angle, η, of the transmitted wave, which is a measure of the difference between the amplitudes of the two circular propagation modes; and the chirality parameter, κ, are calculated by [3]:

$$\theta = \frac{1}{2}\arg\left(\frac{T_R}{T_L}\right), \quad \eta = \frac{1}{2}\tan^{-1}\left(\frac{|T_R|^2 - |T_L|^2}{|T_R|^2 + |T_L|^2}\right),$$

$$\kappa = \log\left(\frac{T_L}{T_R}\right)\frac{1}{j2k_0 d}, \tag{4}$$

where k_0 is the wave vector in the vacuum, and d is the thickness of the sample.

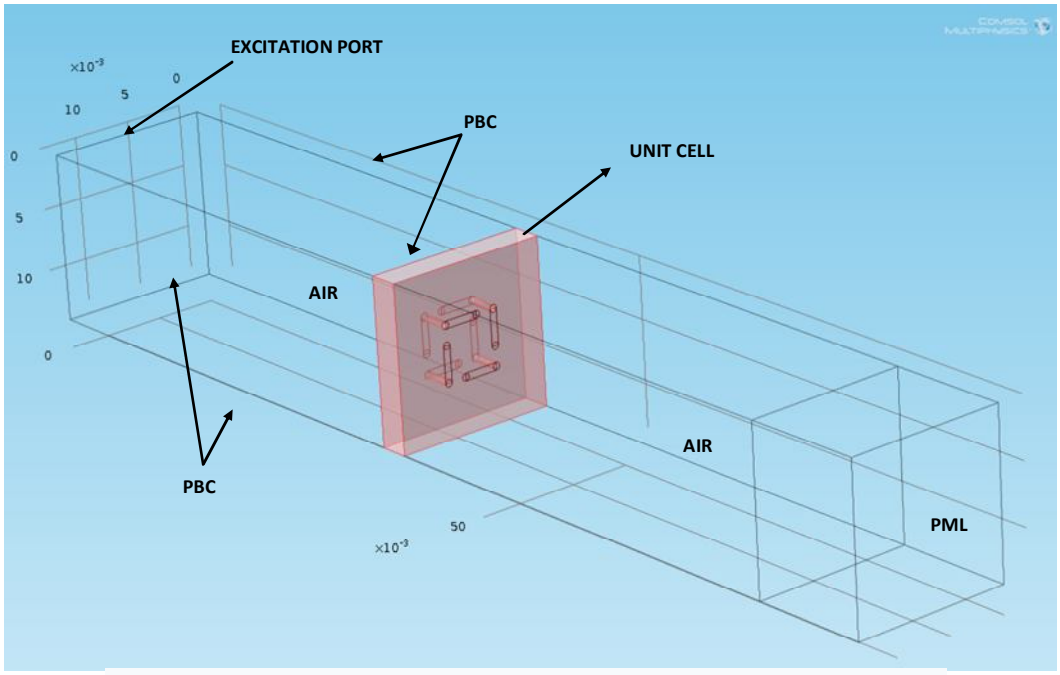

Figure 2. The COMSOL model. PBC: Periodic Boundary Condition. PML: Perfectly matched layer

3. Use of COMSOL Multiphysics

Three-dimensional frequency-domain harmonic propagation mode in RF module of COMSOL is used. We have modeled normal incidence of a TEM plane wave travelling through free space upon one layer of the chiral material (Fig. 1). The incident wave is polarized with the E-field along y-direction and propagation occurs along the positive z-direction. Since the structure is periodic along the interface, it is possible to model an infinite metamaterial slab by a finite-size unit cell, as shown in Fig. 1, and by using Periodic Boundary Conditions (PBC) for the side-walls perpendicular to the propagation direction (in our case, Floquet-PBC have been applied). Geometry, subdomains and boundary conditions are shown in Fig. 2. The incident wave is modeled by using a Port Boundary Condition, which will both launch the incident wave, as well as absorb the reflected wave. The computational domain is truncated by using Perfectly Matched Layer (PML) with Cartesian coordinates. The PML and the unity cell are 1 cm and 2.4 cm thick, respectively, and the whole computational domain spans 9 cm in the direction of propagation, and 1.35 cm in both the x- and y-directions which are the transversal dimensions of the unit cell. Metallic cranks are modeled as empty space surrounded by Perfect Electric Conductor (PEC) walls. All subdomains are set to air except for the FR4 substrate, its conductivity value in COMSOL built-in materials library being modified to 0.08 Sm^{-1} as more suitable for X-band frequencies as regarding experimentally measured losses. Two Cut Point probes are placed 3.5 cm apart from both layers of the unit cell for sampling the x- and y-components of the fields at each frequency of the working range and further manipulation of their values in order to characterize the sample. Mesh size is set to Finer and Copy Mesh option is applied for identical meshing of all periodic boundaries. Frequency-domain STATIONARY-DIRECT-PARDISO parametric solver for 41 frequency values in the range 8-17 GHz is used for fields computation at each frequency. Thus, careful interpolation might be convenient for such a wide-frequency-range dependent functions graphics. The simulations were ran on a PC with a 64-bit Microsoft Windows operating system, with a 3.20 GHz-processor and 30 GB of

RAM. Solutions times were around 2 hours for the entire range of frequencies.

4. Results and Discussion

Fig. 3 shows arrows volume distribution of the–E-field along the axis of the computational domain at the resonance frequency. The linearly polarized incident wave is distorted after transmission through the sample and transformed into left-handed elliptically polarized (circular dichroism). The simulation also shows a strong enhancement of the fields confined inside the sample, which was also reported for non-chiral plasmonic nanostructures at optical frequencies [4, 5]. So, deep inside in this subject would be of interest at microwave frequencies, in particular, in how it depends on the relationship between wavelength and geometry. For example, we have lightly changed the basic structure by closing the connections so as to form a compact parallelepiped and the simulations results show that all the phenomena highlighted herein have disappeared. In order to understand the physical mechanism of the observed behaviour of the material, besides field distribution, simulating the surface current distribution on the structure is further suggested.

Fig. 4 shows, from top to bottom, comparison between experimental (right) and simulated (left) results of the spectra for T_{CO} and T_{CR}, T_L and T_R, θ, and η of the transmitted wave.

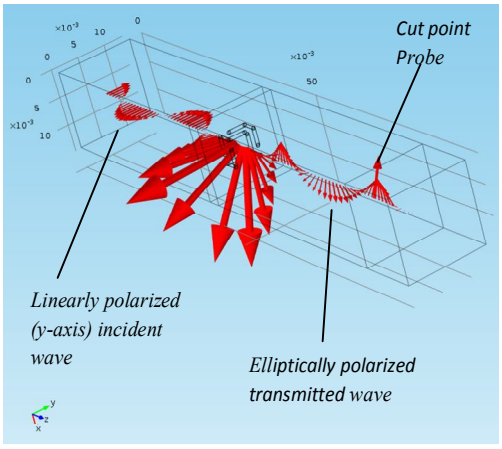

Figure 3. The simulated wave travelling along the axis of the sample (z-axis) at the resonance frequency of 12.04 GHz. Arrows represent the electric field.

The frequency range of the simulated results has been extended beyond the experimental X-band up to 17 [GHz], where two clear resonances at 12.04 GHz and 15.3 GHz are found and we will focus our attention on the first one as the most important. This resonance also appears in the experiment, and it is shifted about 1 GHz. In

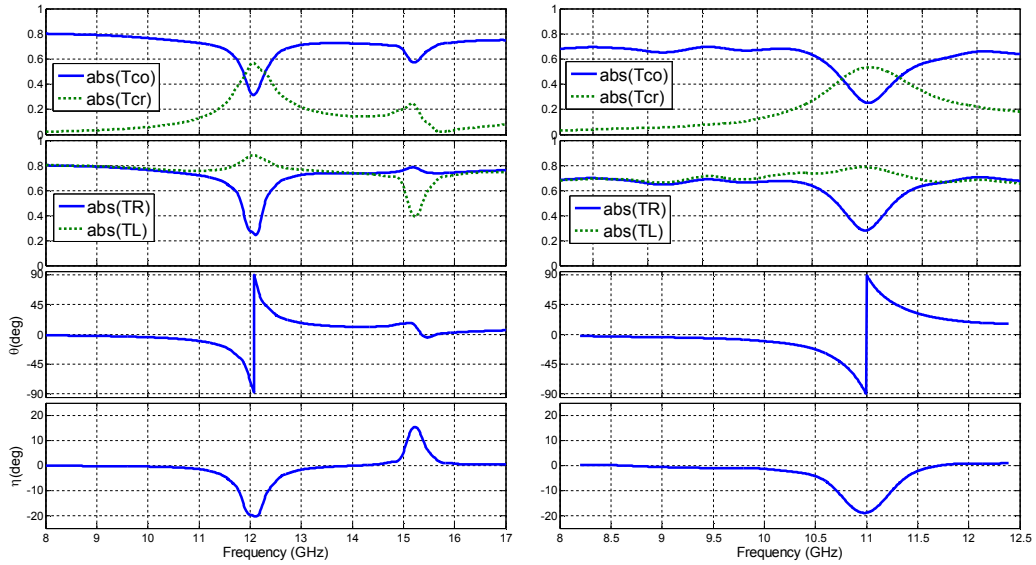

Figure 4. From top to bottom, experimental (right) and interpolated simulated (left) results of T_{CO} and T_{CR}, T_R and T_L, θ, and η for the chiral structura in X-band (experimental) and extended X-band(simulation) frequency ranges (see text for definitions)

spite off this difference, numerical results agree quite well with the experimental ones in describing the phenomenon. Possible reasons for this discrepancy could be due to that the simulated and experimental cranks dimensions and electromagnetic parameters of the substrate might not be the same. At the first resonance, T_L is higher than T_R, and therefore the transmitted wave is left-handed polarized. The effective bandwidth of the resonance is largely determined by the substrate losses. Rotation angle and ellipticity are both resonant at the same frequency, reaching extremes values of about |90º | and |20º|, respectively. The first parameter shows that the transmitted wave is perpendicular to the incident one, and a non zero ellipticity means that the linearly polarized wave is distorted after transmission becoming elliptical. For low frequencies, far from resonance, none of these phenomena happens; between the resonances, the incident wave remains linearly polarized ($\eta \approx 0$) with T_R and T_L being similar, but the polarization plane is rotated about -17º (pure optical activity effects).

Using our experimental free wave technique [6] for characterization of non-chiral materials adapted to chiral ones [7], the transmission and reflection coefficients were measured and effective values for the refractive index, permittivity and permeability were calculated. The experimental results were presented in [1] and here we shown the simulated ones for comparison. The retrieval procedure requires to perform two extra Multiphysics models: first with all materials set to air as a reference of the incident field for the computation of the transmission coefficient and for the extraction of the reflected field out of the total field, and, second, with the incidence interface set as a PEC (short-circuit plate) as a reference to compute the reflection coefficient. For each simulation, both x- and y-polarization components of the field are sampled by using the appropriate Cut Point Probe.

Fig. 5 shows, from top to bottom, the retrieval results for n, κ, n_R, and n_L. Below resonance the refractive index coincides roughly with that of the FR4 substrate and for a narrow frequency bandwidth above the resonance, the effective index is negative, with strong imaginary part associated to material losses. Interpolation is a critical issue in these graphics and, to avoid it, a finer frequency sweep should

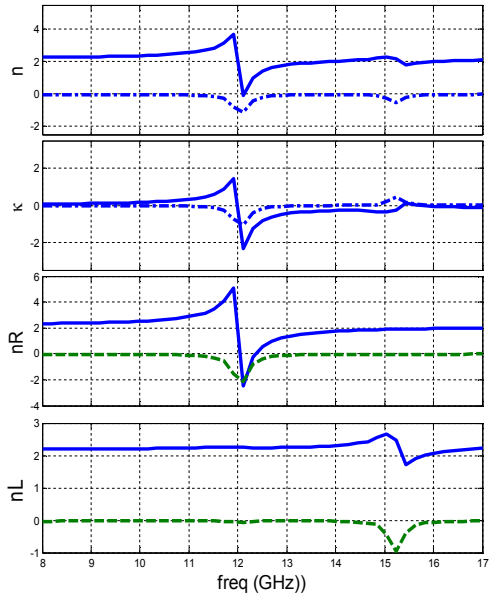

Figure 5. From top to bottom, retrieval simulated values for the refractive index (n), chirality (κ), refractive index of the RCP wave (n_R), and refractive index of the LCO wave (n_L) of the chiral structure as a function of frequency. Solid and dashed lines are real and imaginary values, respectively, of the shown physical quantity.

be carried out around resonance in the model. The chirality parameter peaks at the resonance, where the real part changes the sign from positive to negative. The RCP index n_R, presents a strong dependence with frequency and its real part goes negative within a narrow bandwidth above resonance when $\mathrm{Re}(\kappa)<0$ and $|\mathrm{Re}(\kappa)| > \mathrm{Re}(n)$, as it can be deduced from eq. (2). In contrast with n_R, the LCP index n_L changes slightly with frequency. From the imaginary parts of both refractive indices, we observe that the absorption of the RCP mode is much higher than that of the LCP one, and therefore the transmitted wave is left-handed elliptical polarized (Fig. 3). Alternatively, this phenomenon (circular dichroism) has also been observed by simulating right- and left-handed circularly polarized incident waves, thus a remarkable difference in the transmitted power for each mode was detected as it is shown in Fig. 6. The same conclusions have been obtained in [1] from the experimental results for the same sample.

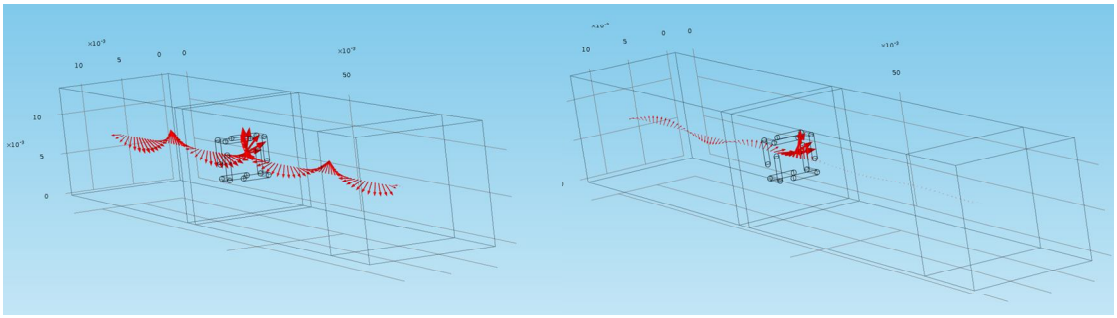

Figure 6. Simulated LCP (left) and RCP (right) waves passing through and being absorbed by the structure, respectively, at the resonance frequency of 12.04 GHz.

5. Conclusions

We have shown that COMSOL RF solver is well suited for the analysis of three dimensional structures with chiral symmetry designed to produce electromagnetic activity at microwave frequencies.

Several models have been implemented in order to reproduce the experimental procedure carried out for the electromagnetic characterization of the material.

The results obtained by the simulation agree quite well with the experimental ones which is an excellent proof of simulation realism provided by COMSOL.

Double Boundary Periodic Condition in three-dimensions has been used as the best option both, to handle with linearly and circularly polarized waves propagating in free space, and to simulate a periodical lattice of chiral metallic cranks.

The simulation has allowed to extend frequency wave range and to implement circularly polarized waves. In addition, simulations can help to visualize the distribution of the field inside the structure which is not possible to be accomplished by means of the experiment.

Further simulation studies have been suggested in order to understand the physical mechanisms of the observed phenomena by using COMSOL potentialities.

6. References

1. Angel J. Garca-Collado et al., Negative refraction of Chiral Metamaterial Based on Four Crank Resonators, *J. Electromagn. Waves and Appl.,* **Vol 26**, 986-995 (2012)

2. J. Li, F.-Q. Yang, and J.-F. Dong, Design and simulation of L-shaped chiral negative refractive index structure, *Progress In Electromagnetic Research,* **Vol. 116**, 395-408 (2011)

3. L. Zhao et al., Conjugated gammadion chiral metamaterials with optical activity an negative index, *Phys. Rev. B,* **Vol. 83**, 035105 (1-4) (2011)

4. Zhengton Liu et al.,Modeling Optical Nanoantenna Arrays with COMSOL Multipyisics, *in Proc.of the COMSOL Conference* (2009 Boston)

5. Manuel Goncalves et al.,Near-fiel in Arrays of Triangular Particles: Coupling Effects and Field Enhancements, *in Proc.of the COMSOL conference* (2011 Boston)

6. J. Muñoz et al., Automatic measurement of permittivity and permeabilityat microwave frequencies using normal and oblique free-wave incidence with focused beam, *IEEE Trans Instrum. Measure.,* **Vol. 47**, *886-892 (1998)*

7. J. Margineda et al. Electromagnetic Characterization of Chiral Media, in Electromagnetic Waves, *Ahmed Kishk (Ed.), ISBN: 980-953-307-527-8, InTech* (2012).

7. Acknowledgements

This work was supported by the Dirección General de Investigación of the Spanish Ministerio de Educación y Ciencia (TEC 2010-21496-C03-02) and by Fundación Séneca Región de Murcia (11844/PI/09).